DE GRAVE, E., DE SITTER, J. & VANDENBERGHE, R. (1975). *Appl. Phys.* **7**, 77–80.
DELAMOYE, P. & MICHEL, A. (1969). *C. R. Acad. Sci. Ser. C*, **269**, 837–838.
HAAS, C. (1965). *J. Phys. Chem. Solids*, **26**, 1225–1232.
HEWAT, A. W. (1979). *Acta Cryst.* A**35**, 248–250.
ISHIKAWA, Y. (1958). *J. Phys. Soc. Jpn*, **13**, 828–837.
JACOB, K. T. & ALCOCK, C. B. (1975). *High Temp. High Pressures*, **7**, 433–439.
KERAMIDAS, V. G., DEANGELIS, B. A. & WHITE, W. B. (1975). *J. Solid State Chem.* **15**, 233–245.
KOSTER, L. & YELON, W. B. (1982). *Neutron Diffraction Newsletter*. ECN Netherlands Energy Research Foundation, Petten, The Netherlands.
LARSON, A. C. & VON DREELE, R. B. (1986). *GSAS – Generalized Structure Analysis System*. Report LA-UR 86-748. Los Alamos National Laboratory, New Mexico, USA.
LIND, M. D. & HOUSLEY, R. M. (1972). *Science*, **175**, 521–523.
NAVROTSKY, A. (1975). *Am. Mineral.* **60**, 249–256.
NAVROTSKY, A. & KLEPPA, O. J. (1967). *J. Inorg. Nucl. Chem.* **29**, 2701–2714.
OKAZAKI, H. (1966). *Jpn J. Appl. Phys.* **5**, 559–560.
PAULING, L. (1930). *Z. Kristallogr.* **73**, 97–112.
POSNJAK, E. & BARTH, T. F. W. (1934). *Z. Kristallogr. Teil A*, **88**, 271–280.
POWELL, R. & POWELL, M. (1977). *Mineral. Mag.* **41**, 257–263.
PREUDHOMME, J. & TARTE, P. (1980). *J. Solid State Chem.* **35**, 272–277.
ROUSE, K. D., COOPER, M. J. & CHAKERA, A. (1970). *Acta Cryst.* A**26**, 682–691.
SABINE, T. M., JORGENSEN, J.-E. & VON DREELE, R. B. (1988). *Acta Cryst.* A**44**, 374–379.
SHANNON, R. D. & PREWITT, C. T. (1969). *Acta Cryst.* B**25**, 925–946.
SMYTH, J. R. (1974). *Earth Planet. Sci. Lett.* **24**, 262–270.
VINCENT, H., JOUBERT, J. C. & DURIF, A. (1966). *Bull. Soc. Chim. Fr.* pp. 246–250.
VIRGO, D. & HUGGINS, F. E. (1975). *Carnegie Inst. Washington Yearb.* **74**, 585–590.
VON DREELE, R. B., JORGENSEN, J. D. & WINDSOR, C. G. (1982). *J. Appl. Cryst.* **15**, 581–589.
WECHSLER, B. A. (1977). *Am. Mineral.* **62**, 913–920.
WECHSLER, B. A., LINDSLEY, D. H. & PREWITT, C. T. (1984). *Am. Mineral.* **69**, 754–770.
WECHSLER, B. A. & NAVROTSKY, A. (1984). *J. Solid State Chem.* **55**, 165–180.
WECHSLER, B. A. & PREWITT, C. T. (1984). *Am. Mineral.* **69**, 176–185.
WECHSLER, B. A., PREWITT, C. T. & PAPIKE, J. J. (1976). *Earth Planet. Sci. Lett.* **29**, 91–103.

Acta Cryst. (1989). B**45**, 549–555

Charge Density of FeF_2

BY M. J. M. DE ALMEIDA, M. M. R. COSTA AND J. A. PAIXÃO

Centro FC1, INIC, Department of Physics, University of Coimbra, 3000 Coimbra, Portugal

(*Received* 14 *September* 1988; *accepted* 17 *July* 1989)

Abstract

The electron density distribution of a rutile-type structure, FeF_2, has been derived from X-ray diffraction measurements carried out on two single crystals at room temperature. Difference density maps were calculated using atomic and temperature parameters refined from high-angle data with $(\sin\theta)/\lambda \geq 0{\cdot}6$ Å^{-1}. The electron populations of $3d$ orbitals were obtained from a least-squares refinement, using model and observed $3d$ structure factors. A comparison is made between these and the results of a multipole refinement. Crystal data: FeF_2, $M_r = 93{\cdot}84$, tetragonal, $P4_2/mnm$, $a = 4{\cdot}7000\ (4)$, $c = 3{\cdot}3100\ (3)$ Å, $V = 73{\cdot}12$ Å^3, $Z = 2$, $D_x = 4{\cdot}2622$ Mg m^{-3}, λ(Mo $K\alpha$) = 0·7017 Å, μ(Mo $K\alpha$) = 49·3 cm^{-1}, $F(000) = 88$, room temperature. Final R values (spherical refinement): 0·010 for 170 reflections from crystal A, 0·012 for 157 reflections from crystal B.

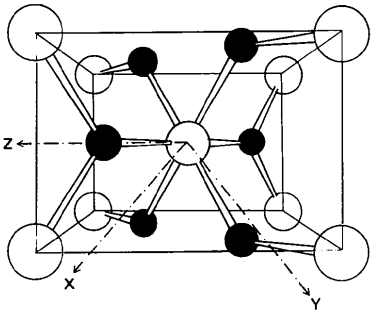

Fig. 1. Unit cell of the rutile structure, showing the directions of the set of axes used in the analysis of $3d$-orbital populations. The open circles represent the positions of Fe atoms and the filled circles those of F atoms.

Introduction

In recent years, several rutile-type structures, MF_2, where M is a transition-metal atom (see Fig. 1), have been examined in our laboratory.

Electrons in the partially filled $3d$ shell of the transition metal 'see' a strong crystal field with a particular symmetry. Consequently, some of the $3d$ orbitals are preferentially occupied, resulting in an aspherical density distribution around the metal atom.

0108-7681/89/060549-07$03.00

The aim of the present work is to determine the degree of asphericity from accurate X-ray diffraction measurements, thus enabling a better understanding of the nature of the metal–ligand bonds.

The results obtained for FeF_2 are discused in this paper and compared with previous work on similar structures (Costa & de Almeida, 1987; Andrade, 1986).

Complementary information about the 3*d* magnetization density in FeF_2 is available from neutron diffraction measurements (de Almeida & Brown, 1988).

Experimental

Two single crystals, *A* and *B*, with approximate dimensions $0{\cdot}10 \times 0{\cdot}11 \times 0{\cdot}12$ and $0{\cdot}07 \times 0{\cdot}08 \times 0{\cdot}11$ mm^3 were selected from a large single crystal kindly supplied by Dr B. Wanklyn (Clarendon Laboratory, Oxford University, England).

The X-ray diffraction measurements were performed on a CAD-4 four-circle diffractometer, at room temperature stabilized to 293 (2) K.

The lattice parameters were determined from 25 reflections with $30{\cdot}4 < 2\theta < 63{\cdot}2°$ for crystal *A* and from 25 reflections with $14{\cdot}5 < 2\theta < 64{\cdot}5°$ for crystal *B* using a standard technique for X-ray diffractometry: $a = 4{\cdot}7000$ (4), $c = 3{\cdot}3100$ (3) Å.

Two sets of data were collected using Mo $K\alpha$ radiation and different crystals. Sets *A* and *B* will refer to data from crystals *A* and *B* respectively.

The total number of reflections and that of independent reflections as well as relevant experimental conditions for each data set are shown in Table 1.

Reflections out to $(\sin\theta)/\lambda = 1{\cdot}1$ Å^{-1} in reciprocal space were measured in ω–2θ scans. Those for which $I_{hkl} \leq 3\sigma_{hkl}$ (σ_{hkl} being the standard deviation of I_{hkl}) were considered to be 'unobserved'.

For each independent reflection up to 16 symmetry-equivalent reflections were measured in order to check the 'efficiency' of the absorption correction applied.

In each experiment, five standard reflections were measured every 3 h. Maximum fluctuations of 4·7% for crystal *A* and 1·5% for crystal *B* were detected; they were attributed to variations in the main-beam intensity (and detector sensitivity) during the exposure time (365 h for experiment *A*, 230 h for experiment *B*). In order to correct for this effect data were rescaled with respect to the standards.

The orientation of the single crystals was checked after every 60 reflections. Whenever the direction of the scattering vector was found to differ more than 10% from that derived from a UB matrix, a set of 4–5 reflections previously selected was measured in order to re-orientate the crystal.

Table 1. *Experimental conditions for the two sets of data collection at* 300 K

	Data set *A*	Data set *B*
Crystal volume (mm^3)	0·0013	0·0006
Radiation	Mo $K\alpha$	Mo $K\alpha$
Scan type	ω–2θ	ω–2θ
Monochromator	Graphite (002)	Graphite (002)
Take-off angle (°)	6·1	6·1
$[(\sin\theta)/\lambda]_{max}$ (Å^{-1})	1·08	1·08
Scan speed (° min^{-1})	0·57–4·14	0·35–4·14
Scan width (°)	1·2–1·6	1·8–2·2
Detector aperture (mm)	(1·9–3·0) × 4·0	(2·1–3·2) × 4·0
Crystal-to-detector distance (mm)	173	173
Total number of reflections	2897	3014
Number of reflections, $I > 3\sigma$	1982	1798
Number of independent reflections	170	157

Data analysis

The analysis of data sets *A* and *B* was performed with the *SDP-Plus* programs (Frenz, 1983), using a PDP11-34 with RSX 11M operating system.

Lorentz and polarization corrections were applied to the integrated intensities of sets *A* and *B*. A ψ-scan absorption correction based on the method described by North, Phillips & Mathews (1968) was applied: six independent reflections were selected with $80 < \chi < 90°$; scans of these reflections and of their geometrically accessible equivalents were made while the crystal was rotated about the scattering vector. Maximum and minimum transmission factors derived from these experimental data were 0·9983, 0·7547 for crystal *A* and 0·9999, 0·9142 for crystal *B*.

The agreement factors for equivalent-reflection intensities were: 2·1% within data set *A*, 3·1% within data set *B*.

Full-matrix least-squares refinements were carried out on $(F_{obs} - F_{calc})^2$, using a non-Poisson contribution weighting scheme based on the following equations:

$$\sigma_{F^2} = [\sigma_I^2 + (pF^2)^2]^{1/2}$$

$$\sigma_F = (\sigma_{F^2})/2F$$

and

$$w = 1/(\sigma_F)^2,$$

where σ_{F^2}, σ_I, σ_F, and w have the usual meanings and p is an experimental instability factor used to down-weight the intense reflections. In the present data analysis, a value of $p = 0{\cdot}04$ was used.

For the calculation of the structure factors F_{calc} a spherical distribution of the atomic electrons was postulated and anomalous-dispersion corrections were made (*International Tables for X-ray Crystallography*, 1974).

The following refinements were carried out with each data set using:

(i) all independent reflections;

(ii) only higher-order data [reflections with $(\sin\theta)/\lambda \geq 0{\cdot}6$ Å^{-1}], to refine a scale factor (S), positional and thermal parameters;

(iii) all independent reflections, fixing all positional and thermal parameters and the scale factor at the refined values (ii), to refine extinction parameter, g.

It is well known that the refinement of the scale factor, positional and thermal vibration parameters should be based on high-order reflection data. In fact, low-angle reflections are the most likely to be affected by extinction, so that their inclusion in a least-squares refinement of the above parameters is liable to introduce undesirable correlations (Stevens & Coppens, 1975).

Hence, only the results obtained in refinements (ii) and (iii) were used in the subsequent analysis.

Refinement (i) including all the observed structure factors [$(\sin\theta)/\lambda \geq 0{\cdot}1$ Å^{-1}] was carried out for comparison of the values thus obtained for the scale factor with those derived from refinement (ii) of the same set of variables. This comparison enables the extent of extinction in both crystals to be roughly estimated.

The extinction parameter g was refined independently [refinement (iii)], using the approximate equation:

$$|F_c| = |F_{\rm obs}|(1 + gI_c),$$

which can be derived from $I_{\rm obs} = I_c\exp(-2gI_c)$ (Stout & Jensen, 1968).

The refinement of anisotropic thermal vibration parameters, U_{ij}, was based on the expression:

$$T = \exp[-2\pi(h^2a^{*2}U_{11} + k^2b^{*2}U_{22} + l^2c^{*2}U_{33} + 2a^*b^*hkU_{12})].$$

The final shift/e.s.d. ratio was smaller than 0·001 for all the parameters refined.

A summary of these refinements is given in Table 2. The positional and thermal parameters (U_{ij}) are shown in Table 3.

The values of calculated and observed structure-factor amplitudes before and after the extinction correction, $F_{\rm calc}$, $F_{\rm obs}$ and $F_{\rm obs}^{\rm corr}$, respectively, are listed in Table 4 for all reflections with $w(F_{\rm calc} - F_{\rm obs}) \geq 2$, where w is the weight of the reflection.

Table 2. *Spherical-atom refinements carried out with data sets A and B*

	(i)		(ii)		(iii)	
Refinement	*A*	*B*	*A*	*B*	*A*	*B*
Range of $(\sin\theta)/\lambda$ (Å^{-1})	> 0·1	> 0·1	> 0·6	> 0·6	> 0·1	> 0·1
Number of reflections used	170	157	127	115	170	157
R	3·3%	3·5%	0·8%	1·0%	1·0%	1·2%
wR	4·2%	4·7%	1·1%	1·5%	1·3%	1.7%
S	0·123 (3)	0·221 (4)	0·116 (1)	0·207 (1)	0·116 (1)	0·207 (1)
$g \times 10^5$	—	—	—	—	4·141 (6)	3·563 (70)

Table 3. *Positional and thermal parameters* (Å^2) *obtained from least-squares refinements, using reflections with* $(\sin\theta)/\lambda \geq 0{\cdot}6$ Å^{-1} *from data sets A and B*

	Data set *A*	Data set *B*
Atom F		
x	0·30122 (11)	0·30141 (17)
U_{11}	0·01294 (10)	0·01318 (15)
U_{33}	0·00838 (13)	0·00907 (22)
U_{12}	−0·00584 (18)	−0·00638 (24)
Atom Fe		
U_{11}	0·00716 (2)	0·00706 (3)
U_{33}	0·00535 (4)	0·00578 (5)
U_{12}	−0·00119 (5)	−0·00130 (9)

Table 4. *Calculated and observed structure factors uncorrected* (F_{obs}) *and corrected* (F_{obs}^{corr}) *for extinction*

	Crystal *A*				Crystal *B*		
hkl	$F_{\rm obs}$	$F_{\rm calc}$	$F_{\rm obs}^{\rm corr}$	*hkl*	$F_{\rm obs}$	$F_{\rm calc}$	$F_{\rm obs}^{\rm corr}$
110	33·40	46·17	46·97	110	35·25	46·16	47·55
011	28·48	32·23	33·03	011	27·67	32·18	31·46
020	17·94	18·71	18·71	111	20·91	22·87	22·15
111	21·21	22·95	22·90	121	33·96	39·36	38·36
121	33·23	39·36	38·25	220	38·58	44·07	44·40
220	36·64	44·15	43·10	002	41·90	51·72	50·56
002	41·50	51·93	51·57	112	29·03	31·80	31·02
130	25·08	26·16	26·45	031	37·24	41·58	41·39
112	29·11	31·91	31·46	330	28·37	29·82	29·57
031	36·93	41·61	41·73				
330	27·91	29·80	29·28				

Charge-density results

The results of Fourier analysis of data sets *A* and *B* are shown as difference density maps drawn for two sections of the unit cell in Figs. 2(*a*), 2(*b*), 4(*a*) and 4(*b*). The corresponding error maps are represented in Figs. 3(*a*), 3(*b*), 5(*a*) and 5(*b*). The standard deviation of the constant regions is 0·11 e Å^{-3} in Figs. 3(*a*), 3(*b*) and 0·17 e Å^{-3} in Figs. 5(*a*), 5(*b*).

The main features that can be observed in identical sections for different crystals show marked similarities.

On the section perpendicular to the c axis, a significant negative density is observed along the lines joining two nearest neighbours (Fe–F) indicating a deficient electron density in these directions. The 'missing' charge appears to be preferentially distributed along the [001] direction, between two nearest (Fe–Fe) neighbours. This can be seen on the section (110).

The significant contour levels observed were assumed to be due to the asphericity of the 3*d*-electron distribution caused by the particular symmetry of the crystalline field.

Charge-density models

Two alternative descriptions of the observed charge densities in FeF_2 were attempted, based on 3*d* atomic orbitals and mulitpole functions.

(*a*) 3*d* atomic orbitals

On the assumption made at the end of the previous section, the difference density may be compared with that deduced from 3*d* atomic orbitals.

In rutile structures, the negative ions (F^-) which constitute the environment of the metal ion occupy the corners of a slightly distorted octahedron. This justifies the assumption of tetragonal symmetry for the (orthorhombic) crystal field. In this case the five $3d$ orbitals, d_{z^2}, $d_{x^2-y^2}$, d_{xy}, d_{xz} and d_{yz} of e_{g_1}, e_{g_2}, t_{2g_1}, t_{2g_2} and t_{2g_3} symmetry are not all independent, but the last two are symmetry equivalent (for the definition of axes, see Fig. 1). Consequently, only the occupancies α_1, α_2 and α_3 of d_{z^2}, $d_{x^2-y^2}$ and d_{xy} orbitals, respectively, were refined independently and $\alpha_4 = \alpha_5 = \frac{1}{2}[1 - (\alpha_1 + \alpha_2 + \alpha_3)]$ were taken as equal populations of the d_{xz} and d_{yz} orbitals, respectively.

The comparison of the difference density observed in FeF_2 and that derived from this model was performed in terms of structure factors, as described elsewhere (Costa & de Almeida, 1987), using the radial form factors listed in *International Tables for X-ray Crystallography* (1974).

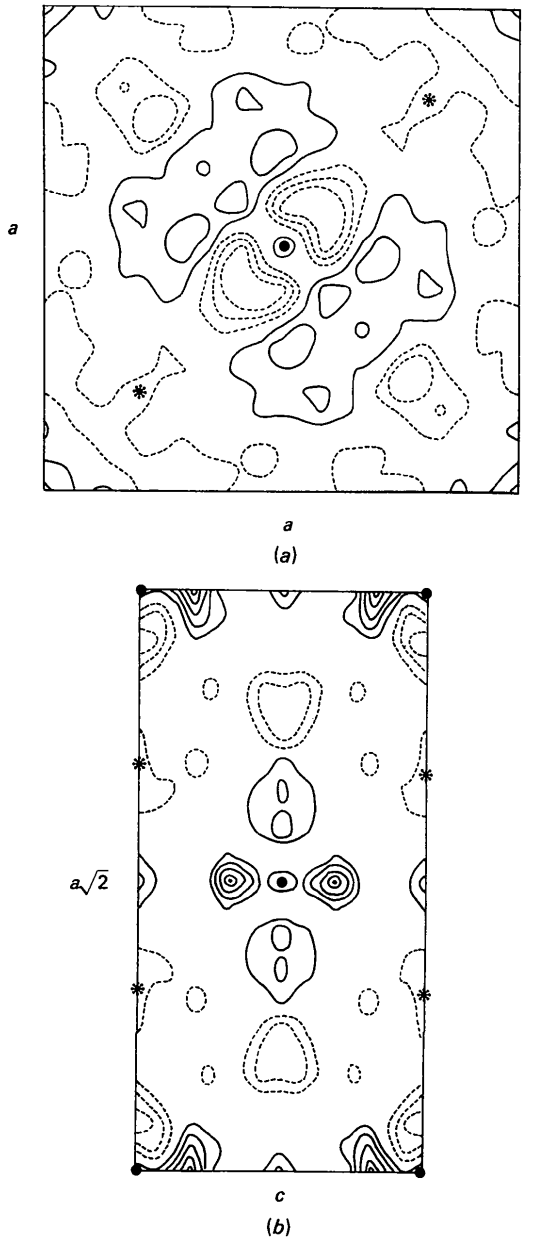

Fig. 2. Difference Fourier maps of FeF_2 (crystal *A*). The contour interval is 0·1 e Å^{-3}; solid and dashed lines represent positive and negative contours, respectively. (*a*) (001) section; (*b*) (110) section. • Fe atoms; * F atoms.

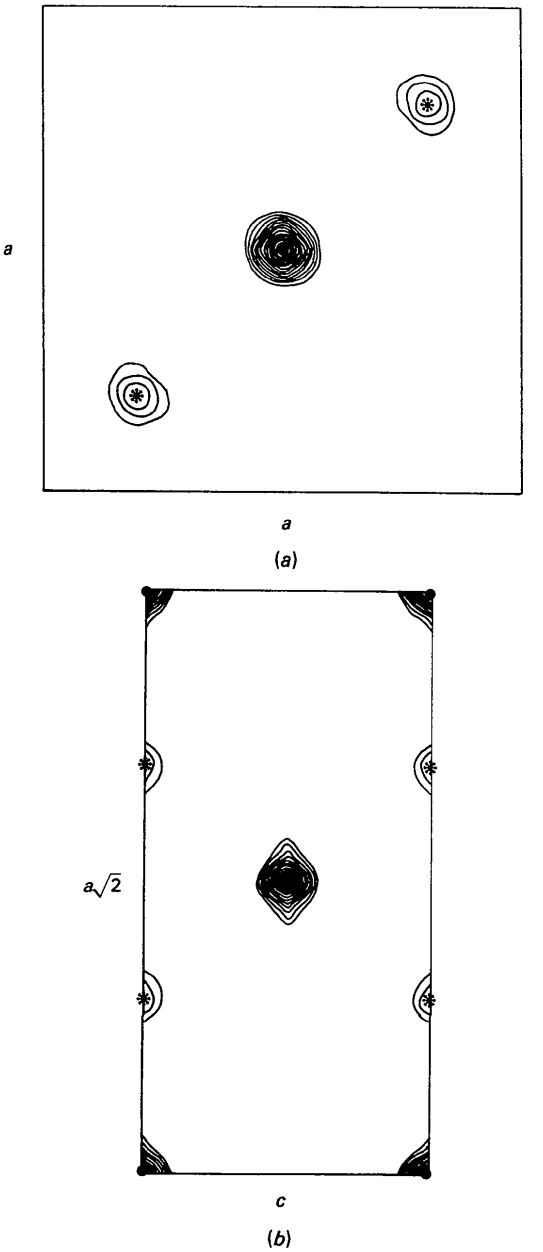

Fig. 3. Fourier maps representing the distribution of errors in FeF_2 (crystal *A*). The contour interval is 0·2 e Å^{-3}. (*a*) (001) section; (*b*) (110) section. • Fe atoms; * F atoms.

The results obtained from data sets *A* and *B* are shown in Table 5(*a*).

The χ^2 parameters for spherical (χ_s^2) and aspherical (χ_a^2) refinements were calculated as:

$$\chi_s^2 = \sum_{hkl}[(F_{obs} - F_{calc}^{sph})/\sigma_{hkl}]^2/(N_v - N_p)$$

and

$$\chi_a^2 = \sum_{hkl}\{[F_{obs} - (F_{calc}^{sph} + F_{calc}^{asph})]/\sigma_{hkl}\}^2/(N_v - N_p),$$

where F_{obs} is the scaled observed structure factor for each independent reflection *hkl* and F_{calc}^{sph} is the corresponding structure factor on the basis of a spherical electron distribution. F_{calc}^{asph} is the calculated aspherical contribution to each F_{calc}^{sph} from the 3*d* electrons of the transition-metal ion. N_p and N_v represent the number of observations (170 reflections from crystal *A* and 157 from crystal *B*) and the number of refined parameters, respectively.

The results obtained from the previous analysis indicate that the asphericity in the electron distribution of FeF_2 is just above the significance level.

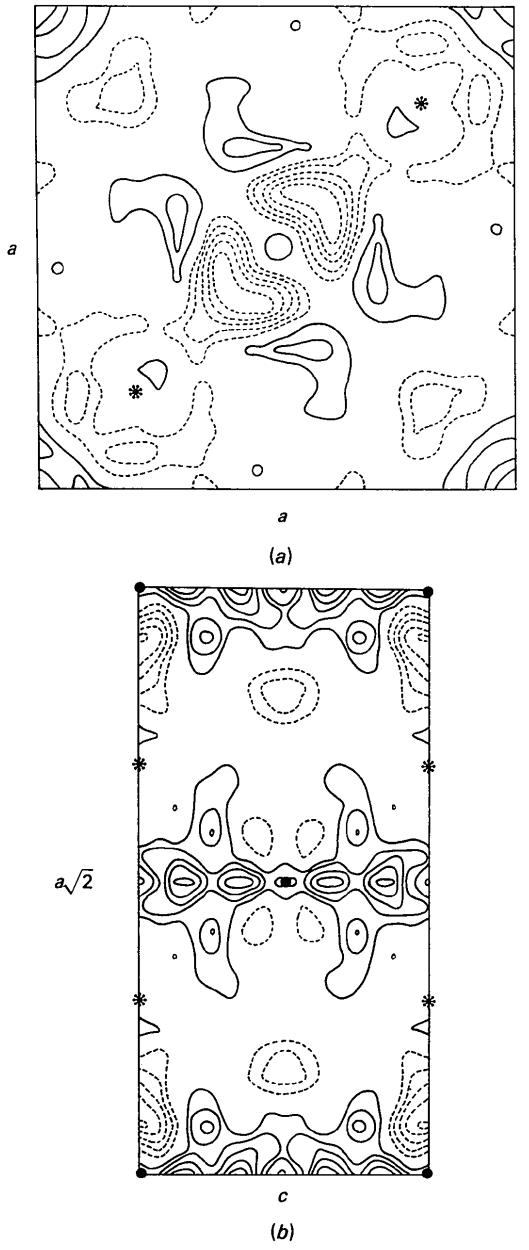

Fig. 4. Difference Fourier maps of FeF_2 (crystal *B*). The contour interval is 0·1 e Å^{-3}; solid and dashed lines represent positive and negative contours, respectively. (*a*) (001) section; (*b*) (110) section. • Fe atoms; * F atoms.

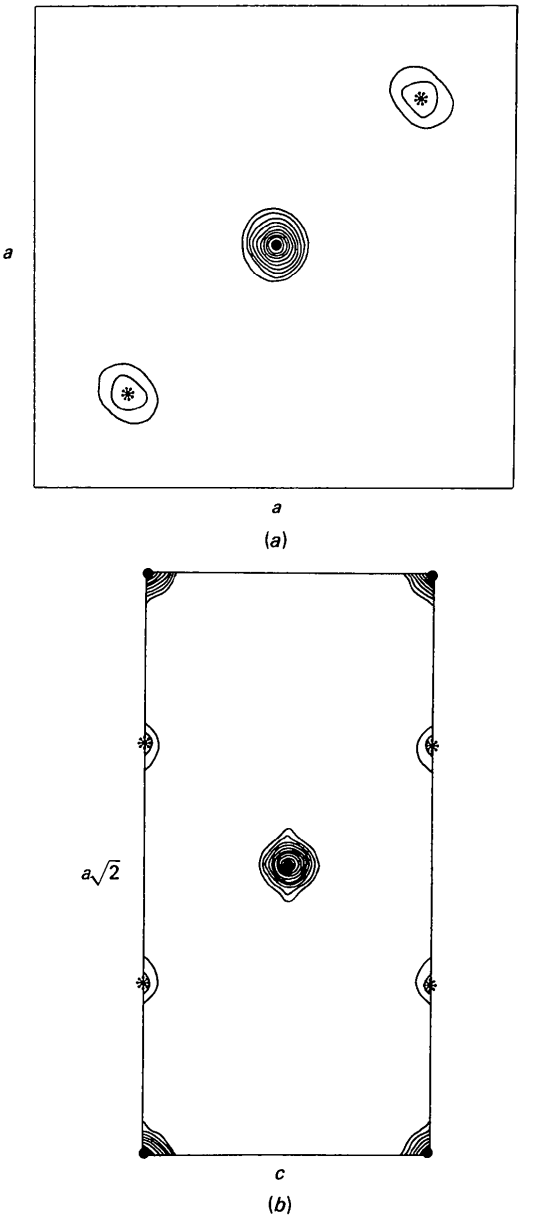

Fig. 5. Fourier maps representing the distribution of errors in FeF_2 (crystal *B*). The contour interval is 0·2 e Å^{-3}. (*a*) (001) section; (*b*) (110) section. • Fe atoms; * F atoms.

Table 5. *Fractional occupancy of the 3d orbitals*

(*a*) Least-squares refinement

	α_1	α_2	α_3	$\alpha_4 = \alpha_5$	χ^2_{sph}	χ^2_{asph}
Crystal *A*	0·203 (17)	0·204 (15)	0·238 (15)	0·178 (23)	5·7	5·2
Crystal *B*	0·196 (25)	0·187 (22)	0·230 (22)	0·193 (35)	1·1	1·2

(*b*) Derived from multipole refinement

	α_1	α_2	α_3	α_4	α_5
Crystal *A*	0·186 (13)	0·259 (14)	0·218 (14)	0·189 (16)	0·193 (16)
Crystal *B*	0·152 (15)	0·274 (17)	0·182 (17)	0·164 (21)	0·206 (21)

Table 6. *Results of the multipole refinement*

U in Å^2.

Crystal *A*		Crystal *B*	
Atom Fe	Atom F	Atom Fe	Atom F
U_{11} = 0·00725 (6)	x = 0·30130 (7)	U_{11} = 0·00714 (7)	x = 0·30130 (11)
U_{33} = 0·00530 (7)	U_{11} = 0·01326 (10)	U_{33} = 0·00552 (3)	U_{11} = 0·01346 (16)
U_{12} = −0·00065 (8)	U_{33} = 0·00866 (10)	U_{12} = −0·00076 (18)	U_{33} = 0·00944 (20)
	U_{12} = −0·00617 (13)		U_{12} = −0·00649 (22)
P_{00} = 0·782 (29)	P_{00} = 1·715 (29)	P_{00} = 0·732 (7)	P_{00} = 1·768 (7)
P_{20} = −0·027 (4)		P_{20} = −0·034 (6)	
P_{22} = 0·006 (4)		P_{22} = −0·007 (5)	
P_{40} = 0·004 (2)		P_{40} = −0·008 (5)	
P_{42} = −0·007 (2)		P_{42} = −0·013 (5)	
P_{44} = 0·013 (2)		P_{44} = 0·029 (5)	
S = 8·843 (29)		S = 4·904 (13)	
MOSC = 21·6′	r = 192 nm	MOSC = 37·9′	r = 109 nm
R = 0·5%	wR = 0·7%	R = 1·0%	wR = 1·2%

The χ^2 value calculated for the aspherical model from crystal data *A* is slightly lower than the corresponding χ^2 value for the spherical model (Table 5*a*).

The spherical refinement from data set *B* yields a χ^2 value close to unity, indicating that no further significant improvement will be attained by trying to fit the observed structure factors with those for an aspherical model of the electron distribution. However, a refinement similar to that carried out for crystal *A* was attempted. Although no improvement could be obtained on the goodness of fit, the occupancy parameters so determined are in very good agreement with those derived for data set *A*.

The results are therefore consistent in showing a very slight preference of the 3*d* electrons of the metallic ion for the t_{2g} orbitals with symmetry d_{xy} with a consequent depletion of the others.

(*b*) *Multipole functions*

The charge density may be alternatively expressed in terms of a superposition of atomic densities, each of which is a series expansion in real spherical harmonics. Based on this description, a set of structure factors can be calculated and compared with the experimental observations.

The comparison was performed for FeF_2 using the least-squares program *MOLLY* (Hansen & Coppens, 1978). This allows the simultaneous refinement of positional, anisotropic vibrational and extinction parameters (mosaic spread, MOSC, and domain radius, r), scale factor and population coefficients corresponding to all multipoles compatible with the local symmetry of the Fe^{2+} ion, up to $l = 4$ (hexadecapoles).

The electron density at any point **r** within the unit cell was taken as

$$\rho_{\text{atomic}}(\mathbf{r}) = \rho_{\text{core}} + \sum_{l=0}^{4} R(r) \sum_{m=-l}^{m=l} P_{lm} Y_{lm}(\mathbf{r}/r),$$

where the term ρ_{core} includes the spherical contribution of the core and valence electrons, *i.e.* $1s^2 2s^2 2p^6 3s^2 3p^6 4s^2$ for Fe or $1s^2$ for F; the term $R(r)P_{00}Y_{00}$ accounts for the distribution of the six electrons ($3d^6$) of the Fe atom, or for the seven electrons ($2s^2 2p^5$) of the F atom. The initial value of P_{00} for each atom is the above number of electrons multiplied by the corresponding multiplicity. The difference between the refined and the initial values of P_{00}(Fe) and P_{00}(F) is a measure of the charge transfer between the two atoms.

The refinement of population parameters P_{lm} was performed in terms of structure factors. Radial form factors calculated by Clementi & Roetti (1974) were used.

No multipole parameters except P_{00} were refined for the F atom. It is reasonable to expect that the main contribution to an eventual asphericity in FeF_2 will come from the 3*d* electrons of the transition-metal element, since the F ion has a closed-shell configuration. Moreover, the increase in the number of variables to refine owing to inclusion of all the symmetry-compatible multipole functions for the F atom, yields an undesirable number of significant correlations.

The results obtained for the two crystals investigated are shown in Table 6. Only two correlations (one for each crystal) were found above 70%, neither of them above 80%

The refined atomic parameters agree within a few standard deviations with those previously obtained (Table 3). The agreement between the two sets of populations is generally satisfactory, the two parameters which come out with different signs for distinct crystals being hardly significant.

Discussion

Generalized relations between multipole population parameters, P_{lm}, and 3*d* orbital occupancies, α_i, have been derived by Holladay, Leung & Coppens (1983), in the form of a 15 × 15 matrix **M** for point group symmetry 1, so that

$$P_{lm\pm} = \mathbf{M}\alpha_i.$$

The dimension of the matrix **M** is smaller for higher point-group symmetries (6 × 6 for point group 4/*mmm*).

The conversion is only valid if the two models are based on the same assumptions. This is not strictly true in the present case, because:

(i) the multipole analysis does allow for charge transfer between the two ions whereas the analysis based on $3d$ orbitals does not;

(ii) the assumption of tetragonal symmetry for the metallic ion surroundings instead of the true orthorhombic one was dropped in the multipole analysis.

However, the results obtained for P_{00} for both atoms show that there is no significant charge transfer. If the multiplicities of the atomic positions are taken into account, the values expected for P_{00} in the absence of charge transfer are 0·75 for Fe and 1·75 for the F atom. In fact,

$$P_{00}(\text{Fe}) = \text{number of } 3d \text{ electrons} \times \text{multiplicity}$$
$$= 6 \times 0{\cdot}125 = 0{\cdot}75$$

and

$$P_{00}(\text{F}) = \text{number of } (2s + 2p) \text{ electrons} \times \text{multiplicity}$$
$$= 7 \times 0{\cdot}25 = 1{\cdot}75.$$

Any increase in one of these values is bound to be accompanied by an equal decrease in the other so as to preserve unit-cell neutrality.

The occupancies of $3d$ orbitals of the Fe^{2+} ion derived from the multilpole population parameters using the appropriate matrix M are given in Table 5(*b*). The comparison of these results with those of Table 5(*a*) shows general agreement within one or (in a few cases) two standard deviations. However, the results derived from the multipole refinement (Table 5*b*) show a significant preference for the $d_{x^2-y^2}$ orbital, whereas those from the refinement of $3d$ occupancies indicate a slight preference for the d_{xy} orbitals. As fewer restrictions are imposed on the multipole model, its results might reproduce better the charge density in the real crystal. However, the conclusion that can be drawn from both models is the preference of the $3d$ electrons for the xy plane, together with a consequent depletion of the d_{z^2}, d_{xz} and d_{yz} orbitals.

We are indebted to the Cultural Service of the German Federal Republic Embassy, the Deutscher Akademischer Austauschdienst (DAAD) and the German Agency for Technical Cooperation (GTZ) for the offer of a CAD-4 automatic diffractometer which enabled the experimental work to be carried out.

References

ALMEIDA, M. J. M. DE & BROWN, P. J. (1988). *J. Phys. C*, **21**, 1111–1127.

ANDRADE, L. C. R. (1986). PhD Dissertation, Univ. of Coimbra, Portugal.

CLEMENTI, E. & ROETTI, C. (1974). *At. Data Nucl. Data Tables*, **14** (3), 4.

COSTA, M. M. R. & DE ALMEIDA, M. J. M. (1987). *Acta Cryst.* B**43**, 346–352.

FRENZ, B. A. (1983). *Enraf–Nonius Structure Determination Package; SDP Users Guide*, version 1.0. Enraf–Nonius, Delft, The Netherlands.

HANSEN, N. K. & COPPENS, P. (1978). *Acta Cryst.* A**34**, 909–921.

HOLLADAY, A., LEUNG, P. & COPPENS, P. (1983). *Acta Cryst.* A**39**, 377–387.

International Tables for X-ray Crystallography (1974). Vol. IV. Birmingham: Kynoch Press. (Present distributor Kluwer Academic Publishers, Dordrecht.)

NORTH, A. C. T., PHILLIPS, D. C. & MATHEWS, F. S. (1968). *Acta Cryst.* A**24**, 351–359.

STEVENS, E. D. & COPPENS, P. (1975). *Acta Cryst.* A**31**, 612–619.

STOUT, G. H. & JENSEN, L. H. (1968). *X-ray Structure Determination*, pp. 410–412. London: Macmillan.

Acta Cryst. (1989). B**45**, 555–562

Structure of the Incommensurately Modulated ε Phase of the Layered Perovskite $[NH_3(C_3H_7)]_2MnCl_4$ (PAMC) at 130 K

BY W. STEURER

Institut für Kristallographie und Mineralogie der Universität, Theresienstrasse 41, *D*-8000 *München* 2, *Federal Republic of Germany*

AND W. DEPMEIER

*Institut für Mineralogie und Kristallographie, BH*1, *TU Berlin, Ernst-Reuter-Platz* 1, *D*-1000 *Berlin* 12, *Federal Republic of Germany*

(*Received* 1 *August* 1988; *accepted* 1 *June* 1989)

Abstract

The incommensurately modulated structure of ε-PAMC has been determined at 130 K: bis-(*n*-propylammonium) tetrachloromanganate(II), M_r = 316·98, superspace group $P^{Abma}_{s11}[0,0{\cdot}363\ (2),0]$, a = 7·436 (4), b = 7·130 (6), c = 25·438 (12) Å, V = 1349 (2) Å^3, Z = 4, D_x = 1·56 Mg m^{-3}, Mo $K\bar{\alpha}$,

0108-7681/89/060555-08$03.00